Inorg. Chem. **2008**, *47*, 9898−9904

High-Pressure Structural and Vibrational Study of $PbZr_{0.40}Ti_{0.60}O_3$

J. Rouquette,*,† J. Haines,† G. Fraysse,† A. Al-Zein,†,‡ V. Bornand,† M. Pintard,† Ph. Papet,† S. Hull,§ and F. A. Gorelli||

Institut Charles Gerhardt UMR CNRS 5253, Université de Montpellier II Sciences et Techniques du Languedoc, Equipe Physico-chimie des Matériaux Organisés Fonctionnels, Place E. Bataillon cc 1503, 34095 Montpellier cedex, France, Laboratoire des Colloïdes, Verres et Nanomatériaux (LCVN), UMR 5587 CNRS, University of Montpellier II, F-34095 Montpellier, France, The ISIS Facility, Rutherford Appleton Laboratory, Chilton, Didcot, Oxfordshire OX11 0QX, United Kingdom, and LENS and INFM, Via Nello Carrara 1, 50019 Sesto Fiorentino, Florence, Italy

Received May 13, 2008

The high-pressure structure and dynamics of $PbZr_{0.40}Ti_{0.60}O_3$ were investigated by means of neutron diffraction, X-ray diffraction, and resonance Raman spectroscopy. The complex (*P*4*mm*, *Cm*, *Cc*, *F*1, *F*$\bar{1}$) phase transition sequence is characterized by these techniques. On the basis of the results of structure refinements, the high-pressure behavior of the spontaneous polarization, the $(Zr,Ti)O_6$ rotation angles, and the polarization rotation angle are obtained. Moreover, resonance Raman spectra combined with previous Raman data in the literature provide evidence that the pressure-induced transition to the monoclinic *Cm* space group and the above transition sequence terminating in a paraelectric state are general features of $Pb(Zr_{1-x}Ti_x)O_3$ ($0.48 \leq x \leq 1$).

Introduction

Due to their technological applications, ferroelectric perovskites exhibiting high piezoelectric coefficients and dielectric constants have attracted the interest of material science researchers over the past 40 years. The most commonly known example of such ferroelectric perovskite solid solutions is the lead zirconate titanate system $Pb(Zr_{1-x}Ti_x)O_3$ (PZT), which is widely used in technological applications such as piezoceramics (piezoelectric transducers and actuators) and thin films (MEMS system or high-frequency devices). A common feature in the temperature-composition phase diagram of these materials is the presence of a morphotropic phase boundary (MPB). Studying the MPB is extremely important, since compounds lying in this region exhibit the highest piezoelectric and electromechanical coupling coefficients. Recently, the MPB has attracted particular attention due to the discovery of a monoclinic phase (*Cm*) separating the rhombohedral from the tetragonal phase ($x \approx 0.48$) at temperatures below 300 K.[1] In this monoclinic form, the polarization can be modulated as, for example, a function of an external applied electric field between the rhombohedral and tetragonal directions based on a polarization rotation mechanism, thus providing a possible explanation for this high piezoelectric response.[2] In addition, a doubling of this monoclinic unit cell was reported at low temperatures ($T \leq 210$ K) for $PbZr_{0.52}Ti_{0.48}O_3$ due to antiferrodistortive tilting of the $(Zr,Ti)O_6$ octahedra based on the appearance of superlattice reflections in electron[3] and neutron diffraction[4] data. Close to the MPB, local structural distortions arise from the static disorder of the zirconium and titanium ion displacements.[5,6] Furthermore, recent experiments based on electron diffraction[5] and

* Author to whom correspondence should be addressed. E-mail: jerome@lpmc.univ-montp2.fr.
† Université de Montpellier II Sciences et Techniques du Languedoc.
‡ Laboratoire des Colloïdes, Verres et Nanomatériaux (LCVN), UMR 5587 CNRS, University of Montpellier II.
§ The ISIS Facility.
|| LENS and INFM.

(1) Noheda, B.; Cox, D. E.; Shirane, G.; Gonzalo, J. A.; Cross, L. E.; Park, S.-E. *Appl. Phys. Lett.* **1999**, *74*, 2059.
(2) Guo, R.; Cross, L. E.; Park, S.-E.; Noheda, B.; Cox, D. E.; Shirane, G. *Phys. Rev. Lett.* **2000**, *84*, 5423.
(3) Noheda, B.; Wu, L.; Zhu, Y. *Phys. Rev. B: Condens. Matter Mater. Phys.* **2002**, *66*, 060103(R)
(4) Hatch, D. M.; Stokes, H. T.; Ranjan, R.; Ragini; Mishra, S. K.; Pandey, D.; Kennedy, B. *J. Phys. Rev. B* **2002**, *65*, 212101.
(5) Glazer, A. M.; Thomas, P. A.; Baba-Kishi, K. Z.; Pang, G. K. H.; Tai, C. W. *Phys. Rev. B: Condens. Matter Mater. Phys.* **2004**, *70*, 184123.
(6) Woodward, D. I.; Knudsen, J.; Reaney, I. M. *Phys. Rev. B: Condens. Matter Mater. Phys.* **2005**, *72*, 104110.

10.1021/ic8008688 CCC: $40.75
Published on Web 10/09/2008

neutron diffraction studies,[7] Raman scattering results,[8] and theoretical calculations[9] have indicated the existence of an intrinsic short-range dynamic disorder over almost the entire PZT solid solution predominantly due to off-center lead displacements.[7,10] Therefore, the boundaries between the different phases, in particular, close to the MPB, are still subject to debate. In a previous study, we investigated the phase transition sequence of $PbZr_{0.52}Ti_{0.48}O_3$ as a function of the temperature by resonance Raman spectroscopy.[11] Using an excitation line of 647.1 nm with an energy close to a self-trapped level exciton energy deficient complex ($Ti_{Ti}'-V_{O}..$) of PZT powder, we induced a resonance effect. The resonance phenomenon resulted in an increase in the phonon intensities, thereby enabling a clear dissociation of the different modes in the Raman spectra, permitting us to detect the structural change of PZT in spite of its well-known static-dynamical disorder. As the physical properties of ferroelectric materials are directly linked to their structure, a better knowledge of the long-range arrangement of PZT is of great interest.

Furthermore, the dielectric constants and piezoelectric coefficients are known to be dependent on three variables (for any given composition): the applied electric field (E), the mechanical stress (σ_{ij}), and the temperature (T).[12] In addition to the ongoing investigation of the relatively well-studied, highly complex, composition-temperature phase diagram of PZT (note also, for example, that careful Rietveld refinements yield significantly better agreement factors using monoclinic models for the long-range structure of $PbZr_{0.60}Ti_{0.40}O_3$, with a *Cc* space group at low temperatures and with a *Cm* space group at high temperatures, rather than the widely accepted rhombohedral symmetry[13]), the effect of hydrostatic pressure is therefore of great importance in order to better understand the dependence of both structural and dielectric properties on the fundamental intrinsic variable P for such a ferroelectric system. Upon increasing pressure, a sequence of low-symmetry structures was identified (*Cm*, *Cc*, *F*1, $F\bar{1}$) in $PbZr_{0.52}Ti_{0.48}O_3$.[14] The high-pressure behavior is consistent with a reduction and a rotation of the spontaneous polarization and the onset of octahedral tilting leading to a doubling of the unit cell. In addition, it was shown for tetragonal $PbZr_{0.40}Ti_{0.60}O_3$ that high pressure can tune the morphotropic phase boundary (associated with the exceptional piezoelectric properties) in the composition-pressure plane to include compositions that do not normally lie in the MPB at ambient pressure.[15] Thus, by controlling the appropriate composition and stress state of materials in ceramics and thin films, optimal piezoelectric properties may be obtained for technological applications. The present complete high-pressure structural and dynamic study of $PbZr_{0.40}Ti_{0.60}O_3$ by neutron diffraction, X-ray diffraction, and resonance Raman spectroscopy provides an important insight into the transition mechanisms at high pressure and provides evidence for a common high-pressure transition sequence in Ti-rich PZT terminating in a paraelectric state.

Experimental Section

The $Pb(Zr_{0.40}Ti_{0.60})O_3$ solid solution was prepared by the conventional solid-state reaction from high-purity (>99.9%) oxides via a two-stage calcination process.[16] Angle-dispersive X-ray diffraction data at high pressure were obtained using a laboratory source and a diamond anvil cell (DAC). The PZT powder was placed in the 150-μm-diameter hole which had been drilled by spark-erosion in a tungsten gasket preindented to a thickness of 100 μm. Powdered ruby or NaCl was added as a pressure calibrant. A 21:4:1 volume ratio methanol/ethanol/H_2O mixture was introduced as a pressure-transmitting medium and remained quasihydrostatic up to 15 GPa. X-ray diffraction patterns were obtained with Zr-filtered Mo radiation from an 800 W microfocus tube. X-ray capillary optics were used, giving a 100-μm-diameter beam. Detection was performed with an imaging plate. Exposure times were typically between 48 and 60 h. The obtained intensities on the imaging plates were integrated as a function of 2θ in order to give conventional, one-dimensional diffraction profiles. Pressures were measured on the basis of the shifts of the ruby R_1 and R_2 fluorescence lines[17] or using the Decker equation of state of NaCl.[18] Cell parameters were obtained either by the Le Bail method or full profile refinement using the software Fullprof.[19] On the basis of our X-ray diffraction patterns, the experimental resolution was not sufficient enough to distinguish small distortion from either tetragonal or cubic symmetry. Pressure−volume data were fitted to the Birch−Murnaghan equation of state (with $B_0' = 4$). High-pressure time-of-flight neutron diffraction data were obtained using a Paris-Edinburgh high-pressure cell at the ISIS spallation source of the Rutherford Appleton Laboratory. The sample was placed in an encapsulated Ti−Zr null scattering gasket with deuterated 4:1 methanol/ethanol as a pressure transmitting medium. The pressure was estimated on the basis fo the pressure-volume data of $Pb(Zr_{0.40}Ti_{0.60})O_3$ obtained from X-ray diffraction. Data were collected at a diffraction angle of $2\theta = 90°$ using a bank of ZnSe scintillators. The acquisition time was on the order of 10 h. The data were normalized with respect to those of a standard vanadium sample and corrected for attenuation due to the tungsten carbide anvils of the pressure cell. Structural refinements were performed with the Rietveld refinement program GSAS.[20] In the refinements, the cell parameters, atomic positions, atomic displacement param-

(7) Corker, D. L.; Glazer, A. M.; Whatmore, R. W.; Stallard, A.; Fauth, F. J. *J. Phys.: Condens. Matter* **1998**, *10*, 6251.
(8) Frantti, J.; Ivanov, S.; Lappalainen, J.; Eriksson, S.; Lantto, V.; Nishio, S.; Kakihana, K.; Rudlöf, H. *Ferroelectrics* **2002**, *266*, 73.
(9) George, A. M.; Iniguez, J.; Bellaiche, L. *Phys. Rev. B: Condens. Matter Mater. Phys.* **2002**, *65*, 180301(R).
(10) Grinberg, I.; Cooper, V. R.; Rappe, A. M. *Nature* **2002**, *419*, 909.
(11) Rouquette, J.; Haines, J.; Bornand, V.; Pintard, M.; Papet, Ph.; Sauvajol, J. L. *Phys. Rev. B: Condens. Matter Mater. Phys.* **2006**, *73*, 224118.
(12) Lines, M. E.; Glass, A. M. *Principles and Applications of Ferroelectrics and Related Materials*; Clarendon: Oxford, U.K., 1977.
(13) Fraysse, G.; Haines, J.; Bornand, V.; Rouquette, J.; Pintard, M.; Papet, Ph.; Hull, S. *Phys. Rev. B: Condens. Matter Mater. Phys.* **2008**, *77*, 064109.
(14) Rouquette, J.; Haines, J.; Bornand, V.; Pintard, M.; Papet, Ph.; Marshall, W. G.; Hull, S. *Phys. Rev. B: Condens. Matter Mater. Phys.* **2005**, *71*, 024112.
(15) Rouquette, J.; Haines, J.; Bornand, V.; Pintard, M.; Papet, Ph.; Bousquet, C.; Konczewicz, L.; Gorelli, F. A.; Hull, S. *Phys. Rev. B: Condens. Matter Mater. Phys.* **2004**, *70*, 014108.
(16) Rouquette, J.; Haines, J.; Bornand, V.; Pintard, M.; Papet, Ph.; Astier, R.; Léger, J. M.; Gorelli, F. *Phys. Rev. B: Condens. Matter Mater. Phys.* **2002**, *65*, 214102.
(17) Mao, H. K.; Xu, J.; Bell, P. M. *J. Geophys. Res.* **1986**, *91*, 4673.
(18) Decker, D. L. *J. Appl. Phys.* **1971**, *42*, 3239.
(19) Rodríguez-Carvajal, J. Unpublished.
(20) Larson, A. C.; Von Dreele, R. B. *GSAS: General Structure Analysis System*; Los Alamos National Laboratory: Los Alamos, NM, 1994.

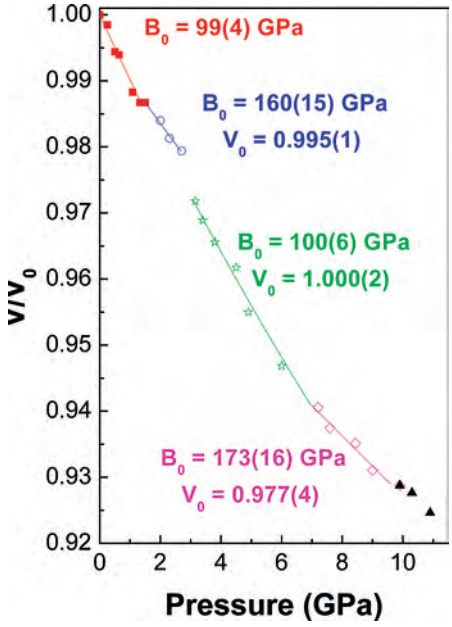

Figure 1. Volume-change vs pressure of $PbZr_{0.40}Ti_{0.60}O_3$ at 298 K. The B_0 values are calculated with the Birch−Murnaghan state equation ($B_0' = 4$).

eters, scale factor, background, and line shape parameters were varied. High-pressure resonance Raman experiments were performed using a Krypton ion laser (647.1 nm), a Jobin-Yvon Model U 1000 double monochromator, and a charge coupled device cooled to 140 K. Samples were loaded in a membrane-type DAC along with a ruby crystal as a pressure calibrant and argon as a pressure-transmitting medium. The laser output powers were around 10 mW.

Results and Discussion

X-Ray Diffraction Results. The unit-cell constants obtained by X-ray diffraction for the tetragonal phase at ambient pressure are in good agreement with previous work for $x = 0.60$. Figure 1 shows the relative volume as a function of pressure for $PbZr_{0.40}Ti_{0.60}O_3$ at 298 K. Three distinct transitions can be detected either by a decrease in compressibility (at 1.5 or 7.1 GPa) or by a 0.8% volume change which occurs at 2.7 GPa. However, one has to note that the 21:4:1 methanol/ethanol/water pressure transmitting medium used in this study becomes viscous at about 10−11 GPa. Therefore, the data obtained above 10 GPa must be treated with caution.

Neutron Diffraction Results. The data reported previously by neutron diffraction on $PbZr_{0.40}Ti_{0.60}O_3$ indicated the presence of the monoclinic structures *Cm* and *Cc* respectively at 2.7 and 4.1 GPa,[15] the same ferroelectric forms which are proposed to be responsible for the high piezoelectric properties characteristic of the MPB composition $PbZr_{0.52}Ti_{0.48}O_3$ at ambient pressure.[15] These phases, *Cm* and *Cc*, which have successive group−subgroup relationships with *P*4*mm* (*P*4*mm* → *Cm* → *Cc*), were considered from the group theoretical analysis of octahedral tilting in ferroelectric perovskites.[21] From Figure 1, the *P*4*mm*−*Cm* transformation is found to occur at around 1.5 GPa; this phase transition was also identified in the same pressure range from

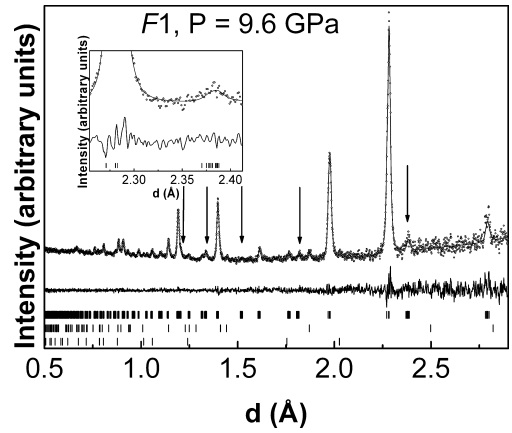

Figure 2. Experimental and calculated profiles from Rietveld refinements of the triclinic *F*1 phase of $PbZr_{0.40}Ti_{0.60}O_3$ at 9.6 GPa (Rwp = 4.9, Rp = 7.3, $\chi^2 = 0.5$). The difference profile is on the same scale. Vertical ticks indicate the calculated positions of the PZT phase (top) and of tungsten carbide (middle) and nickel (bottom) from the anvils of the pressure cell. The strongest superlattice reflection is shown in the inset. Arrows indicate the most prominent superlattice reflections.

the change in slope of the inverse of the dielectric constant ($1/\varepsilon_r'$) as a function of the pressure.[15] The latter *Cm*−*Cc* phase transition can directly be detected by neutron diffraction from the appearance of superlattice reflections (tilt system $a-\ a-\ c-$),[22,23] which continue to increase in intensity up to the highest pressure reached, as shown below, indicating a doubling of the unit cell due to octahedral tilting. The superlattice reflections are due to oxygen displacements and are not detected in X-ray diffraction due to the low-scattering factor of oxygen.

Figure 2 represents the neutron diagram (highest pressure reached from neutron diffraction experiments). Various structural models were used for the refinement of the neutron diffraction pattern of $PbZr_{0.40}Ti_{0.60}O_3$ at 9.6 GPa, Figure 2, including monoclinic *Cc*, rhombohedral *R*3*c*, and triclinic *F*1 space groups. These phases were again considered from the group theoretical analysis of octahedral tilting in ferroelectric perovskites.[21] *R*3*c* (tilt system $a-\ a-\ a-$)[22,23] is a supergroup of *Cc* (tilt system $a-\ a-\ c-$),[22,23] while *F*1 is the direct subgroup of *Cc* (tilt system $a-\ b-\ c-$).[22,23] Note also that the *Cc*−*R*3*c* phase transition is required by Landau theory to be first-order.[21] Of these three structural models, the poorest refinement was obtained using the rhombohedral structure (Rwp = 5.7%, Rp = 8.7%). The 111 reflection should be split for an *R*3*c* structure with a relative intensity ratio of 0.9:1. This intensity ratio does not correspond to the observed data. Similarly, the 200 reflection is not split in rhombohedral symmetry, which thus cannot reproduce the experimental data. Consequently, the *R*3*c* structure is not observed at high pressure for these PZT solid solutions.

The best refinement was obtained using the triclinic model (Rwp = 4.9%, Rp = 7.3%). In such a structure, $(Zr,Ti)O_6$ rotation angles about axes parallel to the pseudocubic **a**, **b** and, **c** directions can be calculated (ω_a, ω_b, ω_c). Additionally, the refined atomic positions can be used to calculate the spontaneous polarization along with the polarization rotation

(21) Stokes, H. T.; Kisi, E. H.; Hatch, D. M.; Howard, C. J. *Acta Crystallogr., Sect. B* **2002**, *58*, 934.
(22) Glazer, A. M. *Acta Crystallogr., Sect. A* **1975**, *31*, 756.
(23) Glazer, A. M. *Acta Crystallogr., Sect. B* **1972**, *28*, 3384.

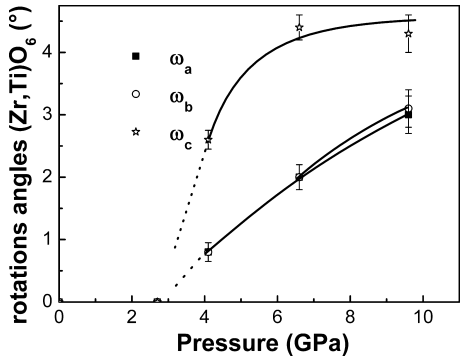

Figure 3. Calculated $(Zr,Ti)O_6$ rotation angles of $PbZr_{0.40}Ti_{0.60}O_3$ as a function of pressure. In the monoclinic *Cc* structure, ω_a and ω_b are equal and become different in the triclinic *F*1 symmetry. Solid lines are a guide for the eyes.

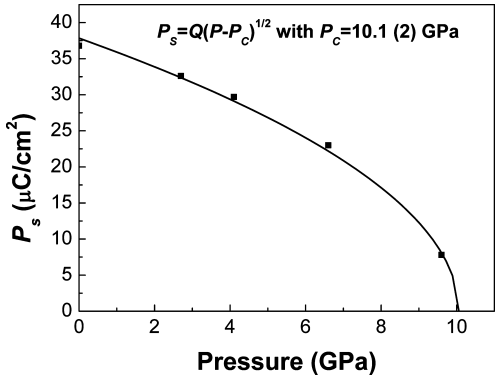

Figure 4. Calculated spontaneous polarization (P_s) as a function of pressure. Extrapolation of $P_s \rightarrow 0$ is obtained using a square-root function characterizing a second-order ferroelectric−paraelectric transformation.[12,24]

angles (θ) with respect to the pseudotetragonal *z* axis in the monoclinic phase using the dipole moment equation $P_s=(1/V)\Sigma_i q_i r_i$.[14] In the triclinic form, ω_a and ω_b, which are identical in *Cc* symmetry, become different, Figure 3, and the spontaneous polarization is described with a second rotation angle φ.

Use of a Paris−Edinburgh high-pressure cell with tungsten carbide anvils limits this work to pressures of about 10 GPa, and thus a paraelectric phase $F\bar{1}$ observed for $PbZr_{0.52}Ti_{0.48}O_3$ was not reached in this neutron diffraction experiment. However, extrapolation of $P_s \rightarrow 0$ using a square-root function characterizing a second-order ferroelectric−paraelectric transformation[12,24] can give a good idea of this critical pressure P_C, Figure 4. The corresponding value is 10.1(2) GPa, in perfect accordance with results obtained from Raman spectroscopy measurements discussed below. By analogy with $PbZr_{0.52}Ti_{0.48}O_3$, the structural transition $F1 \rightarrow F\bar{1}$ is proposed for this ferroelectric−paraelectric transformation.[14] In this previous study, the paraelectric phase was characterized by (1) the shift of the (Zr,Ti) cations toward the center of the $(Zr,Ti)O_6$ octahedra at 5 GPa and (2) the persistence of superlattice reflections due to oxygen displacements (tilt system $a- b- c-$).

The in-plane rotation angle of the spontaneous polarization (θ) increases from 0° in the *P*4*mm* structure to 76° in the *F*1 form, Figure 5. This value is close to the pseudocubic

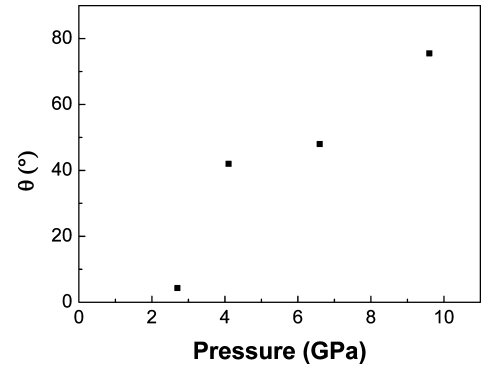

Figure 5. Calculated polarization rotation angle (θ) with respect to the pseudotetragonal *z* axis in the monoclinic phase (pseudocubic [001] direction).

[112] direction previously observed for the polarization vector in the recent study of the *F*1 structure in PLZT ($\theta = 70.5°$),[25,13] indicating that the rotation of the in-plane component of P_s principally occurs between the [001] and [112] directions.

This high-pressure rotation of P_s is found to be a general feature of PZT solid solutions.[14] Finally, the high-pressure compression behavior is dominated by octahedral tilting. This compression mechanism appears at the *Cm*−*Cc* phase transition. The *Cc* phase is characterized by two distinct rotation angles, ω_a and ω_c. These angles increase upon compression and can be followed by the increase in intensity of the superlattice reflections. At the *Cc*−*F*1 phase transition, ω_a and ω_b become distinct, as expected in triclinic symmetry.

Resonance Raman Spectroscopy Results. Beginning from ambient conditions, important changes are observed in the pressure behavior of the Raman modes 1 and 2 of $PbZr_{0.40}Ti_{0.60}O_3$, Figure 6, which correspond respectively to the ferroelectric soft mode [A_1(1TO)] and the [A_1(2TO)] mode. In the tetragonal phase near the transition pressure, the dielectric susceptibility $\chi_{33} \propto 1/\omega^2[A_1(1TO)]$ from the Lyddane−Sachs−Teller equations,[26] which implies that the evolution of the A_1(1TO) mode with increasing *P* will give information on the particular high-pressure ferroelectric behavior of such a solid solution. On the basis of a high-pressure Raman spectroscopic study, it was reported that both modes soften in $PbTiO_3$ (the lead titanate end member), implying a second-order transition to a paraelectric cubic, high-pressure phase.[27] However, these results have to be revised, as Foster et al. later found[28] that the mode energies and symmetry assignments were not correct: the energy of the lowest-frequency A_1(TO) mode is higher than the energy of the lowest E(1LO) mode at 300 K.[28,29] It follows that, contrary to what was reported, these are the E(1TO) and E(1LO) modes, which soften simultaneously around 12 GPa in $PbTiO_3$, and not the E(1TO) and A_1(1TO) originating from the F_{1u}(1TO) mode in the cubic phase.[27] This implies a

(24) Samara, G. A.; Peercy, P. S. *Solid State Phys.* **1981**, *36*, 1.
(25) Liu, H.; Harrison, R.; Putnis, A. *J. Appl. Phys.* **2001**, *90*, 6321.
(26) Lyddane, R. H.; Sachs, R. G.; Teller, E. *Phys. Rev.* **1941**, *59*, 673.
(27) Sanjurjo, J. A.; López-Cruz, E.; Burns, G. *Phys. Rev. B: Condens. Matter Mater. Phys.* **1983**, *28*, 7260.
(28) Foster, C. M.; Li, Z.; Grimsditch, M.; Chan, S.-K.; Lam, D. J. *Phys. Rev. B: Condens. Matter Mater. Phys.* **1993**, *48*, 10160.
(29) Garcia, A.; Vanderbilt, D. *Phys. Rev. B: Condens. Matter Mater. Phys.* **1996**, *54*, 3817.

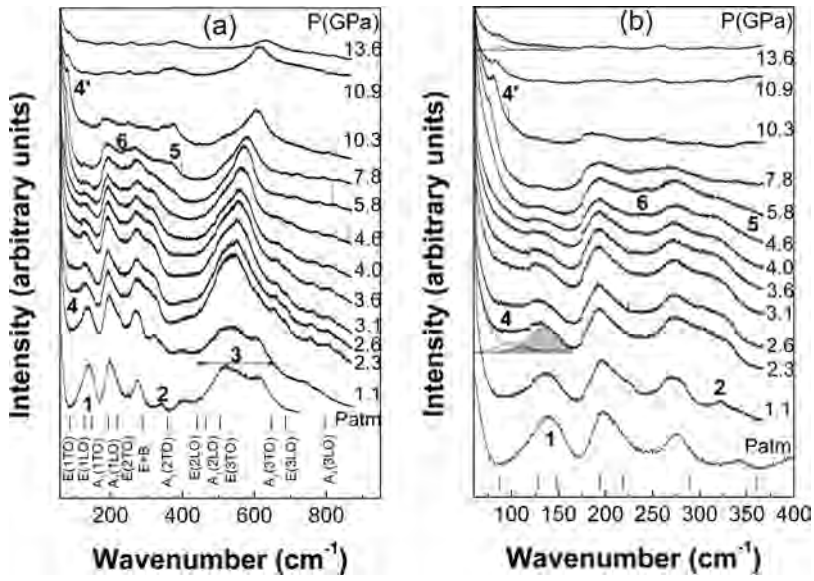

Figure 6. (a) Raman spectra of $PbZr_{0.40}Ti_{0.60}O_3$ as a function of pressure. Phase transitions can be detected from the pressure behavior of the Raman signals 1−6.[15] (b) Plots of the 60−400 cm^{-1} region of the Raman spectra in order to better distinguish the disappearance of mode 1 and the softening of 4 replaced by 4′ upon increasing the pressure. Fitting of the modes 1 and 4 to Voigt functions (gray and white, respectively) are shown at 2.3 and 13.6 GPa. Positions and assignments of the Raman peaks at room temperature for $PbTiO_3$ are indicated (ref 26).

second-order transformation between two ferroelectric phases and not a ferroelectric−paraelectric (cubic) phase transition as previously mentioned.[27] As soft modes at the Γ point have E-mode irreducible representation, it means that the high-pressure phase of $PbTiO_3$ will be linked to a reduction in symmetry. From first-principles calculations, Wu and Cohen also found that, at 0 K, pressure induced condensation only of the E(1TO) phonon, which gave rise to a transition to the monoclinic structure (space group *Cm*),[30] which is the same observed in the morphotropic phase boundary of PZT.[1] In Raman studies of PZT solid solutions, as no single crystals are available, assignment of the phonons is not possible and analysis of the Raman modes has to be performed by analogy with the Ti-rich end member: $PbTiO_3$. Thus, it was necessary to first take into consideration the high-pressure Raman spectroscopy study of $PbTiO_3$ by Sanjurjo et al.,[27] reporting a second-order phase transition to a cubic paraelectric state at $P_c \approx 12$ GPa. As mentioned above, as mode energies and symmetry assignments were later revised,[28] the transformation to the paraelectric form has to be reconsidered and replaced by a transition to a monoclinic phase as calculated by Wu and Cohen.[30] From our Raman spectra, Figure 6, the transformation to the monoclinic phase already identified by neutron diffraction can be detected, as in the case of $PbTiO_3$, from the softening of modes 1 and 2 ($[A_1(1TO)]$, $[A_1(2TO)]$), which abruptly change in behavior between 1.1 and 2.3 GPa;[15] above 2.3 GPa, these modes harden upon compression. Additionally, region 3, which is dominated by vibrations of O^{2-} anions (stretching and bending of $(Zr,Ti)O_6$ octahedra), becomes more intense and more symmetric due to the coalescence of vibrations centered around 540 cm^{-1}. The Raman spectrum at 2.3 GPa is also characterized by the appearance of mode 4, which in the present case of a tetragonal−monoclinic phase transition (*P*4*mm*−*Cm*) can initiate from the loss of degeneracy of the E phonon (in C_{4v}^1 symmetry), leading to splitting into $A' + A''$ modes. On the basis of Raman spectroscopic results, it is therefore proposed that the Ti-rich $Pb(Zr_{1-x}Ti_x)O_3$ ($0.48 \leq x \leq 1$) exhibits a pressure-induced transition to the monoclinic *Cm* structure.[15,30,31]

Upon increasing pressure, modes 5 and 6 appear in the Raman spectra, Figures 6. These changes are clearly associated with the phase transition between the two monoclinic phases (*Cm*−*Cc*).[32−34] The increase in the number of modes at the phase transition is consistent with the greater number of modes predicted by group theory due to the doubling of the unit cell. This transition was found to be strongly first-order from X-ray diffraction, Figure 1, associated with a 0.8% volume change, which occurs at 2.7 GPa. Note that, although there is a group−subgroup relationship between *Cm* and *Cc*, this phase transition can be either first- or second-order. Such a volume change can easily be explained by a higher compressibility of the doubled monoclinic unit cell, Figure 1, due to the additional compression mechanism characterized by the rotation of the oxygen octahedra. As a first-order transition is characterized by its kinetics, it can explain the progressive increase in intensity of the 5 and 6 Raman bands upon compression, which are clearly detected only around 4.6 GPa, Figure 6. The *Cc*−*F*1 transformation found by neutron diffraction can also be detected from the softening of mode 4, which is replaced around 6 GPa by 4′, which is narrower and more intense, Figures 6b and 7a. Note that mode 5 associated with the $(Zr,Ti)O_3$ rotation[32] increases in intensity with increasing pressure, providing additional

(30) Wu, Z.; Cohen, R. E. *Phys. Rev. Lett.* **2005**, *95*, 037601.
(31) Rouquette, J.; Haines, J.; Bornand, V.; Pintard, M.; Papet, Ph.; Gorelli, F. A. *J. Eur. Ceram. Soc.* **2005**, *25*, 2393.
(32) Mihailova, B.; Bismayer, U.; Güttler, B.; Gospodinov, M.; Konstantinov, L. *J. Phys.: Condens. Matter* **2002**, *14*, 1091.
(33) Haines, J.; Rouquette, J.; Bornand, V.; Pintard, M.; Papet, Ph.; Gorelli, F. A. *J. Raman Spectrosc.* **2003**, *34*, 519.
(34) Rouquette, J.; Haines, J.; Bornand, V.; Pintard, M.; Papet, Ph.; Bonnet, B.; Gorelli, F. A. *Solid State Sci.* **2003**, *5*, 451.

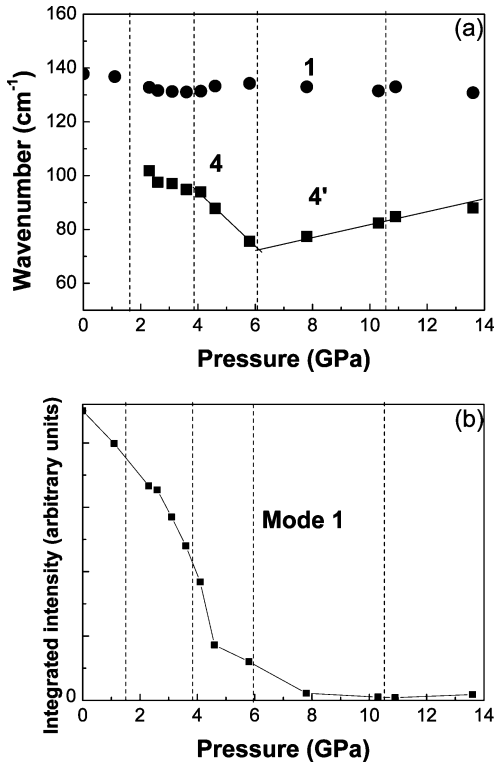

Figure 7. (a) Raman shifts and (b) integrated intensities of modes 1 and 4(′) as a function of pressure obtained from fitting with Voigt functions.

evidence that the high-pressure behavior of PZT is characterized by antiphase octahedral tilting.[14] Finally, as described by the Lyddane−Sachs−Teller equations,[26] the transition to the paraelectric form ($F\bar{1}$) is found to occur around 10.5 GPa from the disappearance of mode 1 (A_1(1TO)), Figures 6b and 7b. The strong Raman spectrum observed in the paraelectric phase is also in agreement with triclinic $F\bar{1}$ symmetry, as such a spectrum is not forbidden by group theory, as it is in the case of the $Pm\bar{3}m$ cubic space group. As mentioned above, the ferroelectric behavior of $Pb(Zr_{0.40}Ti_{0.60})O_3$ can be linked to the pressure evolution of mode 1 (A_1(1TO)), Figure 7. Note that in Figure 1b of our previous report,[15] we fitted the behavior of the A_1(1TO) mode with two functions, as this phonon is well-known to have an asymmetric line shape.[35] In the present Figure 6, we fitted this phonon using a simple Voigt function in order to follow its average width and Raman shift. By following both the Raman shift and the integrated intensity of this fundamental polar ferroelectric phonon, one can easily detect the different phase transitions and the transformation to the paraelectric state. Note that even at the highest pressure reached, this mode 1 does not completely disappear, Figure 6b. On the basis of our neutron diffraction data, the transition to the paraelectric state is consistent with an $F1-F\bar{1}$ phase transition. On the basis of Raman selection rules, mode 1 (A_1(1TO)) must be Raman-inactive in a triclinic nonpolar state. The observed activity of this mode can be explained by possible random off-center displacements of the titanium atom; the use of resonance Raman spectroscopy in our case focuses on the energy close to a self-trapped level exciton energy-deficient complex ($Ti_{Ti}'-V_{O}..$) linked therefore to titanium displacements. This off-center position of titanium in the paraelectric state has already been reported in $PbTiO_3$ as a function of temperature by the persistence above T_c of the pre-edge feature at the Ti K-edge in X-ray absorption spectra.[36] It was found that the persistence of this off-center displacement is consistent with the presence of an order−disorder component in the dynamics of $PbTiO_3$, which displays a soft mode and a dielectric constant typical of displacement-type ferroelectrics. Therefore, from this resonance Raman spectroscopy study, one can also identify, as in the X-ray absorption spectroscopy technique, an order−disorder component in the ferroelectric−paraelectric phase transition of $Pb(Zr_{0.40}Ti_{0.60})O_3$ as a function of pressure. Additionally, the paraelectric spectrum at 13.6 GPa, Figure 6, is half as intense as that at 10.9 GPa. Note that we previously reported that the resonance behavior using the 647.1 nm excitation line is structure-dependent.[11] The intensity change can, therefore, be related to the evolution of the resonance conditions and thus to the electronic levels involved as a function of the phase transition sequence in PZT materials. Thus, the change in Raman intensity can clearly be a signature of a phase transition. The present example permits this hypothesis to be confirmed.

On the basis of the above remarks, the recently reported enhancement of ferroelectricity in $PbTiO_3$ perovskites and related materials as a function of pressure[37] needs to be reconsidered. In this recent study, the authors used the earlier mode assignments of Burns and Scott,[38] which were later revised by Foster et al.[28] Therefore, these authors observed the simultaneous softening of the E(1TO) and E(1LO) modes around 12 GPa and not the E(1TO) and A_1(1TO) modes as originally proposed. On the basis of Raman data,[39] one can follow the pressure behavior of the A_1(1TO) mode, which hardens with pressure (as in $Pb(Zr_{0.40}Ti_{0.60})O_3$ in our present study) and gradually decreases in intensity until it disappears around 30 GPa, providing evidence of a ferroelectric−paraelectric phase transition. Note also that, contrary to what was earlier reported by Sanjurjo et al., the Raman spectra did not disappear either above 12 GPa, which was taken as clear evidence of a transition to a cubic paraelectric form,[43] or at the highest pressure reached (about 38 GPa; as in $Pb(Zr_{0.40}Ti_{0.60})O_3$ in our present study). This is clearly consistent with recent X-ray absorption spectroscopy measurements, which showed that the Ti atoms are still displaced from the center of their octahedral site above the critical pressure $P_C \sim 12$ GPa,[40] corresponding to the supposed transition to a paraelectric state.[27,37] On the basis of the revised mode assignments, this would instead correspond to a ferroelectric tetragonal−monoclinic phase transition. In

(35) Seong, M. C.; Hyun, M. J.; Kim, T.-Y. *Phys. Rev. B: Condens. Matter Mater. Phys.* **2001**, *64*, 014103.
(36) Sicron, N.; Ravel, B.; Yacoby, Y.; Stern, E. A.; Dogan, F.; Rehr, J. J. *Phys. Rev. B: Condens. Matter Mater. Phys.* **1994**, *50*, 13168.
(37) Kornev, I. A.; Bellaiche, L.; Bouvier, P.; Janolin, P.-E.; Dkhil, B.; Kreisel, J. *Phys. Rev. Lett.* **2005**, *95*, 196804.
(38) Burns, G.; Scott, B. A. *Phys. Rev. B: Condens. Matter Mater. Phys.* **1973**, *7*, 3088.
(39) Janolin, P.-E. Ph.D. thesis, 2006.
(40) Jaouen, N.; Dhaussy, A. C.; Itié, J. P.; Rogalev, A.; Marinel, S.; Joly, Y. *Phys. Rev. B: Condens. Matter Mater. Phys.* **2007**, *75*, 224115.

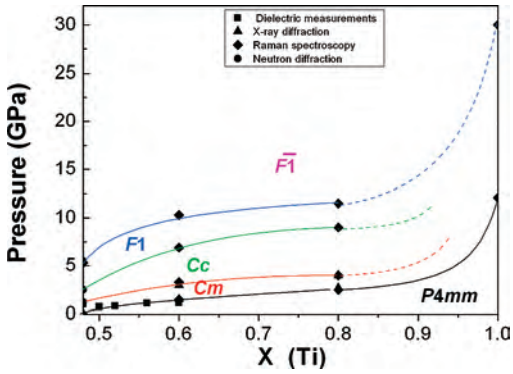

Figure 8. Pressure-composition diagram of $Pb(Zr_{1-x}Ti_x)O_3$ ($0.48 \leq x \leq 1$). The solid lines represent phase boundaries obtained from X-ray diffraction, Raman spectroscopy, and dielectric measurements. The *P*4*mm*−*Cm* transformation pressure of $PbTiO_3$ is based on the Raman data of Sanjurjo et al.[27] and the mode assignments of Foster et al.[28] The ferroelectric−paraelectric phase-transition pressure is based on recent Raman results.[39]

addition to their experimental high-pressure Raman spectra, Kornev et al. argued that the enhancement of ferroelectricity arises from an increase in the cell parameter ratio $c/a > 1$ above $P_C \sim 12$ GPa.[37] As mentioned above, a transformation to a monoclinic phase can easily explain this ratio.

Finally, the present study combined with previous work enables us to construct a pressure-composition phase diagram of $Pb(Zr_{1-x}Ti_x)O_3$ ($0.48 \leq x \leq 1$), Figure 8. This diagram is characterized by the presence of five different phases (i.e., *P*4*mm*, *Cm*, *Cc*, *F*1, and $F\bar{1}$). As discussed above, we propose the pressure-induced transformation to the monoclinic *Cm* structure as a general feature of this PZT solid solution in the investigated composition range. On the basis of Raman data,[39] the ferroelectric−paraelectric phase transition in $PbTiO_3$ can be situated at about 30 GPa from the progressive disappearance of the A_1(1TO) mode in accordance with the Lyddane−Sachs−Teller relationship.[26]

Conclusions

The complex (*P*4*mm*, *Cm*, *Cc*, *F*1, $F\bar{1}$) phase transition sequence of $Pb(Zr_{0.40}Ti_{0.60})O_3$ was investigated under high pressure by neutron diffraction, X-ray diffraction, and resonance Raman spectroscopy. From the neutron data and the corresponding refined atomic positions, the spontaneous polarization, the $(Zr,Ti)O_6$ rotations angles, and the polarization rotation angle were studied as a function of pressure. As in $Pb(Zr_{0.52}Ti_{0.48})O_3$,[14] the high-pressure behavior was found to be consistent with a reduction and a rotation of the spontaneous polarization and the onset of octahedral tilting leading to unit cell doubling. Using the present Raman resonance data and the previously reported high-pressure Raman spectra of Sanjurjo et al.,[27] we propose that the pressure-induced transition to the monoclinic *Cm* space group is a general feature of $Pb(Zr_{1-x}Ti_x)O_3$ ($0.48 \leq x \leq 1$). This particular transformation for $PbTiO_3$ is based on the simultaneous softening of the E(1TO) and E(1LO) modes around 12 GPa and not the E(1TO) and A_1(1TO) modes as originally proposed. Note that the pressure-induced rotation of the spontaneous polarization obtained on the basis of the *P*4*mm*−*Cm* transformation originally proposed in PZT[15] was further observed for $PbTiO_3$ films under tensile stress[41] and $PbTiO_3$ under compressive stress.[42] Our result requires a reconsideration of the recently reported enhancement of ferroelectricity in $PbTiO_3$ perovskites and related materials as a function of the pressure.[37] From the experimental Raman data of these authors,[39] it appears that the ferroelectric−paraelectric phase transition of $PbTiO_3$ takes place at close to 30 GPa from a progressive disappearance of the ferroelectric A_1(1TO) mode, and even at the highest pressure reached (40 GPa), no reappearance of the A_1(1TO) mode was observed as clear evidence of the reappearance of ferroelectricity, which would result in local repulsion between overlapping charge densities of the Ti 3d−e_g O 2s orbitals.[37] The reappearance of ferroelectricity under pressure in $PbZn_{1/3}Nb_{2/3}O_3$ with a diffuse *C*2/*c*−*Cc* phase transition[43] appears less likely, as there is clearly no experimental evidence for the reappearance of polar information from Raman spectroscopy and X-ray diffraction.

Acknowledgment. The authors acknowledge the European Union supporting LENS under Contract No. RII3-CT-2003-506350.

IC8008688

(41) Catalan, G.; Janssens, A.; Rispens, G.; Csiszar, S.; Seeck, O.; Rijnders, G.; Blank, D. H. A.; Noheda, B. *Phys. Rev. Lett.* **2006**, *96*, 127602.
(42) Budimir, M.; Damjanovic, D.; Setter, N. *J. Appl. Phys.* **2007**, *101*, 104119.
(43) Janolin, P.-E.; Dkhil, B.; Bouvier, P.; Kreisel, J.; Thomas, P. A. *Phys. Rev. B: Condens. Matter Mater. Phys.* **2006**, *73*, 094128.